1984

Mass Spectrometric Studies of Oxygen Isotope Exchange Reactions with Oxide Surfaces

Gayle J. Allen
Old Dominion University

ABSTRACT

MASS SPECTROMETRIC STUDIES OF OXYGEN ISOTOPE EXCHANGE REACTIONS WITH OXIDE SURFACES

Gayle J. Allen

Old Dominion University, 1984

Director: Dr. Billy T. Upchurch

Isotopic exchange reactions with the surface of amorphous silica and crystalline quartz were studied mass spectrometrically. A mixture of approximately 2% $^{18}O_2$ in neon was used as the test gas, and was passed over the surface of the oxides. Measurements were taken as a function of temperature and residence time, for kinetic studies.

These studies clearly show a second order rate law for the surfaces examined. The rate constant on amorphous silica was 2.2×10^{2} L/mol/sec. The energy of activation was 35.3 kcal/mol and the frequency factor was 1.35×10^{9} L/mol/sec. On the crystalline quartz the rate constant was 2.0×10^{2} L/mol/sec. The energy of activation was 65.2 kcal/mol and the frequency factor was 4.52×10^{2} L/mol/sec.

The postulated mechanism for a bimolecular

reaction would occur at temperatures above that required for dehydroxylation. This allows chemisorption of a molecule of $^{18}O_2$ to form a bridged six-membered ring upon which a subsequent collision of a second $^{18}O_2$ molecule results in an oxygen isotope exchange.

ACKNOWLEDGEMENTS

The author wishes to express her sincere thanks and gratitude to George Wood and NASA Langley for the opportunity to work on this project.

The author wishes to extend special thanks to Billy T. Upchurch for his patience and guidance throughout my course of study.

A very special thanks to my husband, for without his support, understanding and typing skills, this endeavor would never have seen completion.

TABLE OF CONTENTS

Page

LIST OF FIGURES v

LIST OF TABLES vi

Chapter

I. INTRODUCTION 1

II. EXPERIMENTAL 7

A. APPARATUS AND MATERIALS 7

B. PROCEDURE 12

C. EXPERIMENTAL DATA 17

1. REACTION OF OXYGEN-16 AND OXYGEN-18 BLANK 17

2. REACTION OF OXYGEN-16 AND OXYGEN-18 ON QUARTZ WOOL 21

3. REACTION OF OXYGEN-16 AND OXYGEN-18 ON CRYSTALLINE QUARTZ 21

4. REACTION OF OXYGEN-16 AND OXYGEN-18 ON AMORPHOUS SILICA 23

5. REACTION OF OXYGEN-16 AND OXYGEN-18 ON BOROSILICATE GLASS WOOL.....26

6. REACTION OF OXYGEN-18 BLANK 26

7. REACTION OF OXYGEN-18 WITH CRYSTALLINE QUARTZ.....26

8. REACTION OF OXYGEN-18 WITH AMORPHOUS SILICA 29

9. REACTION OF OXYGEN-18 WITH PYREX TUBE AND BOROSILICATE GLASS WOOL.....29

Page

10. REACTION OF NITROGEN-14 AND NITROGEN-15 ON CRYSTALLINE QUARTZ AND AMORPHOUS SILICA 29

D. CRYSTALLOGRAPHIC STUDIES 31

E. KINETIC STUDIES 31

III. RESULTS AND DISCUSSION.....38

IV. CONCLUSION 44

BIBLIOGRAPHY 46

LIST OF FIGURES

FIGURE PAGE

1. Schematic Diagram of Analysis System 8
2. Schematic Diagram of Flow System 10
3. Spectrum of Neon Effluent 13
4. Spectrum of $^{16}O_2$ $^{18}O_2$ in Neon 15
5. Spectrum Showing Appearance of m/e 34 16
6. Spectrum of $^{18}O_2$ in Neon 18
7. Spectrum Showing Isotopic Exchange with the Surface 19
8. Spectrum of $^{14}N_2$ and $^{15}N_2$ in Neon 20
9. Isotopic Oxygen Exchange on Quartz Wool 22
10. Isotopic Oxygen Scrambling on Crystalline Quartz 24
11. Isotopic Oxygen Scrambling on Amorphous Silica 25
12. Isotopic Oxygen Scrambling on Borosilicate Glass Wool 27
13. Isotopic Oxygen Exchange with Crystalline Quartz 28
14. Isotopic Oxygen Exchange with Amorphous Silica 30
15. Graph of Kinetic Studies Data on Amorphous Silica 39
16. Graph of Kinetic Studies Data on Crystalline Quartz 40

LIST OF TABLES

TABLE		PAGE
I.	Characteristics of Clear Fused Silica	9
II.	Kinetic data for Oxygen-18 at 1000°C on Amorphous Silica	34
III.	Kinetic data for Oxygen-18 at 1100°C on Amorphous Silica	35
IV.	Kinetic data for Oxygen-18 at 1000°C on Crystalline Quartz	36
V.	Kinetic data for Oxygen-18 at 1100°C on Crystalline Quartz	37

CHAPTER I

INTRODUCTION

A high speed vehicle flying at altitudes above 96 kilometers encounters both free oxygen and nitrogen atoms which have been produced by cosmic radiation. These atoms tend to recombine on the catalytic surface of the vehicle and cause serious heating problems on re-entry. Such vehicles require a thermal protection barrier that prevents excessive heating by reflecting, dissipating, or otherwise preventing the accumulation of too much external heat on atmospheric re-entry.

For many years the thermal protection of the surface of entry vehicles from space was via ablative heat shields. In ablation the heat generated from atmospheric friction, chemical reactions, and atomic recombinations is dissipated by pyrolysis of the heat shield material and the corresponding loss of its mass via the formation of gaseous or fragmented products.

Thermal protection for NASA's shuttle orbiter, however, is achieved through the use of ceramic tiles. The tiles now in use are made up of 99.8% pure silica and while providing thermal protection are very fragile, bulky, and geometrically unique. For example, 34,000 ceramic tiles were used on the space

shuttle Columbia to protect it from the heat of re-entry.

Two kinds of silica tiles have been used on the space shuttle Columbia and Challenger. Approximately 90% of the tiles are made up of a material weighing nine pounds per cubic foot. The other 10% of the tiles are much denser, weighing 22 pounds per cubic foot. These are placed where higher temperatures are observed on the shuttle; and while they are tougher and more durable, the increased weight decreases the payload. Recently a composite of silica and aluminum borosilicate fibers has been developed having a weight of 12 pounds per cubic foot. These composites are more rigid and stronger than previous materials. These are fabricated by welding the borosilicate fibers to the silica fibers.[1] Measured temperatures are above that which would be expected from atmospheric friction, indicating that the surface does have some catalytic properties. The ideal material for a thermal protective shield would have a relatively non-catalytic surface, a high emissivity, be durable, and provide a low weight loading of the vehicle. It must adhere to a metal surface and be relatively stable both physically and chemically when exposed to high temperatures. Thus it is necessary to evaluate to what extent the current material is catalytically involved

with atmospheric components under re-entry temperature conditions, and find a method which can be used to evaluate the potential of other materials to be considered for use as relatively non-catalytic overcoats.

PROPOSED WORK

In earlier studies, Linnett and Marsden[2] investigated the kinetics for the recombination of oxygen atoms on glass surfaces using a 2450 megahertz microwave discharge for atom generation. Reactions were monitored by thermocouple measurement of the heat given off when the atoms recombined. It was concluded that on a borosilicate glass surface the reaction was first order. For salt surfaces such as potassium chloride and lithium chloride the atom recombination was also found to be first order. Greaves and Linnett later studied twenty-eight surfaces[3,4,5] including oxides and halides in the same manner. They observed exponential decay of atom concentration down the side of the tube in their experimental apparatus and that the measured activities could not be attributed to any one factor associated with the surface of the material.

As early as 1955, Kistiakowsky and others[6] studied the kinetics of N_2 afterglow using a mass spectrometer. In 1957 they studied nitrogen atoms

further[7] by observing reactions involving oxides of nitrogen. Rate constants were calculated but mechanisms were not determined. Klein and Herron[8] used mass spectrometry to obtain rate constants and mechanisms for gas phase reactions of oxygen atoms with NO, NO_2, and O_2. Winter[9] has evaluated some oxide surfaces and the isotopic exchange of molecular oxygen using mass spectrometry.

The kinetics and mechanism for the adsorption and subsequent desorption with exchange or recombination of O_2 and N_2 are still not fully understood for gas-silica type systems. In order to assess and evaluate a material for non-catalytic characteristics it is necessary to better understand the basic mechanisms and parameters upon which exchange or recombination can depend.

It has been suggested that there are "active sites" on the surface of SiO_2 or other such materials which allow exchange or recombination to take place. If an experimental technique could be found which would enable one to measure the number of "active sites" available on these types of surfaces and the mechanism involved, it would provide a means to more readily select a more inert material for a non-catalytic overcoat for metal surfaces.

In this study it was proposed to conduct an

investigation on the behavior of oxygen and nitrogen molecules in dissociation, recombination, and/or exchange reactions with the surface of selected silica materials as a function of temperature. Molecules were to be used instead of atoms to determine whether their behavior was similar to the well documented behavior of the atomic state.

It was proposed that the possible reactions of oxygen molecules on selected silica-type surfaces be studied using $^{16}O_2$ and $^{18}O_2$ isotopes. The possible reactions which may take place between these molecules and the oxide surfaces would be monitored using a magnetic deflection mass spectrometer. A reaction would result in isotopic scrambling of a mixture of $^{16}O_2$ and $^{18}O_2$. Initially there would be two peaks at m/e 32 and m/e 36 with a gradual appearance of a peak at m/e 34 representing the scrambled molecule $^{16}O^{18}O$:

$$^{16}O_{2(g)} + {}^{18}O_{2(g)} \xrightarrow{Si^{16}O_{2(s)}} 2{}^{16}O^{18}O_{(g)} + Si^{16}O_{2(s)}.$$

If exchange occurred with the surface of the oxide materials, it could be examined by the appearance of m/e 34 occurring when only $^{18}O_2$ gas was being passed over the oxide surface. This could be shown as:

$$^{18}O_{2(g)} \xrightarrow{Si^{16}O_{2(s)}} Si^{16}O^{18}O_{(s)} + {}^{16}O^{18}O_{(g)}$$

In this effort the above reactions were

monitored and kinetic data was used to better define a mechanism for the reactions.

CHAPTER II

EXPERIMENTAL

Apparatus and Materials

All measurements were made on a Dupont CEC 21-104 magnetic sector mass spectrometer using a stainless steel capillary for continuous introduction of samples. The spectrometer has a 12.7 cm radius, and is a 180^{o} magnetic sector of the Dempster type. A schematic diagram of the analysis system is given in Figure 1.

The crystalline quartz, (lot number 32145), was obtained from International Minerals and Chemical Corporation as a 50/140 mesh powder with a stated purity of 99.9%. This was sieved and the 60/80 mesh fraction with a BET area of $0.097 m^2/gm$ was used. The BET areas of both the crystalline quartz and amorphous silica were determined by Porous Materials Inc.

The amorphous silica (lot number 1976) was purchased from Davidson Company as silica gel. The 28/200 mesh material was sieved and the 60/80 mesh fraction was heated to $1150^{o}C$ to convert it to amorphous silica prior to use. The BET area was $0.052 m^2/gm$.

FIGURE 1

SCHEMATIC DIAGRAM OF ANALYSIS SYSTEM

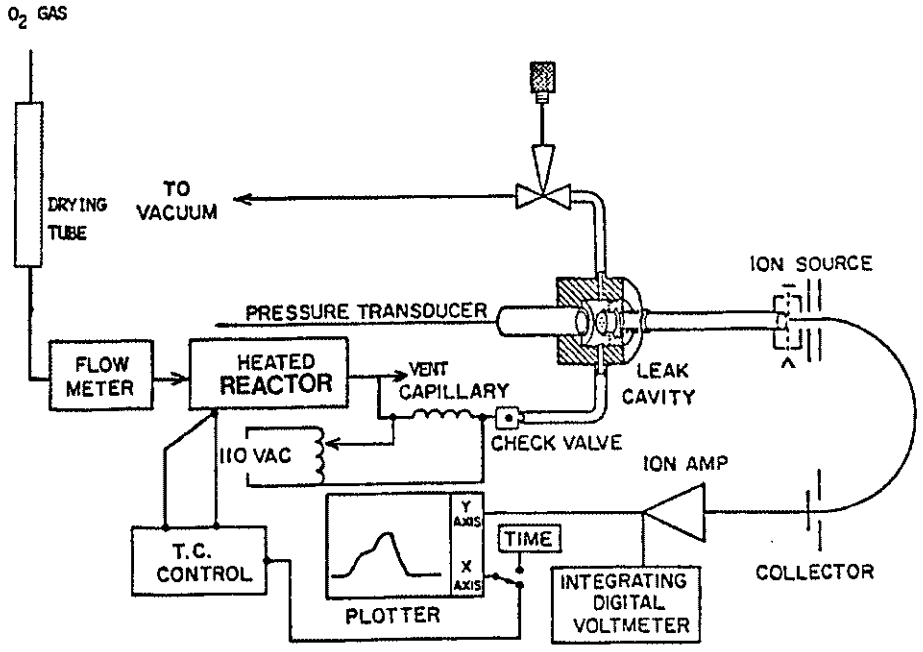
O_2 GAS
DRYING TUBE
TO VACUUM
ION SOURCE
PRESSURE TRANSDUCER
FLOW METER
HEATED REACTOR
VENT CAPILLARY
LEAK CAVITY
CHECK VALVE
110 VAC
ION AMP
T.C. CONTROL
Y AXIS
X AXIS
TIME
PLOTTER
INTEGRATING DIGITAL VOLTMETER
COLLECTOR

Ace Glass Incorporated was the source of the high purity quartz wool. This was chosen when it was determined that the glass wool contained numerous contaminants and had a softening point well below the operating temperature of the experiment. The diameter of the quartz wool fibers was 0.6 microns.

The fused quartz tubes used to contain the materials of interest were obtained from stock in the glass shop at NASA Langley. Table I lists some characteristics of the fused quartz.[11,12,13]

Table 1.

Characteristics of Clear Fused Silica

A.	Prepared by fusion of natural quartz
B.	Natural quartz purity 99.97 - 99.98% SiO_2
C.	Fused quartz purity 99.8% SiO_2
D.	Physical Characteristics
	1. Fusing Point 1750°C
	2. Annealing Point 1140°C
	3. Highly resistant to thermal shock
	4. Prolonged use above 1000°C results in devitrification

The experimental flow system schematic is shown in Figure 2. The flow system was plumbed with one-eighth inch o.d. copper tubing and was assembled to

FIGURE 2

SCHEMATIC DIAGRAM OF FLOW SYSTEM

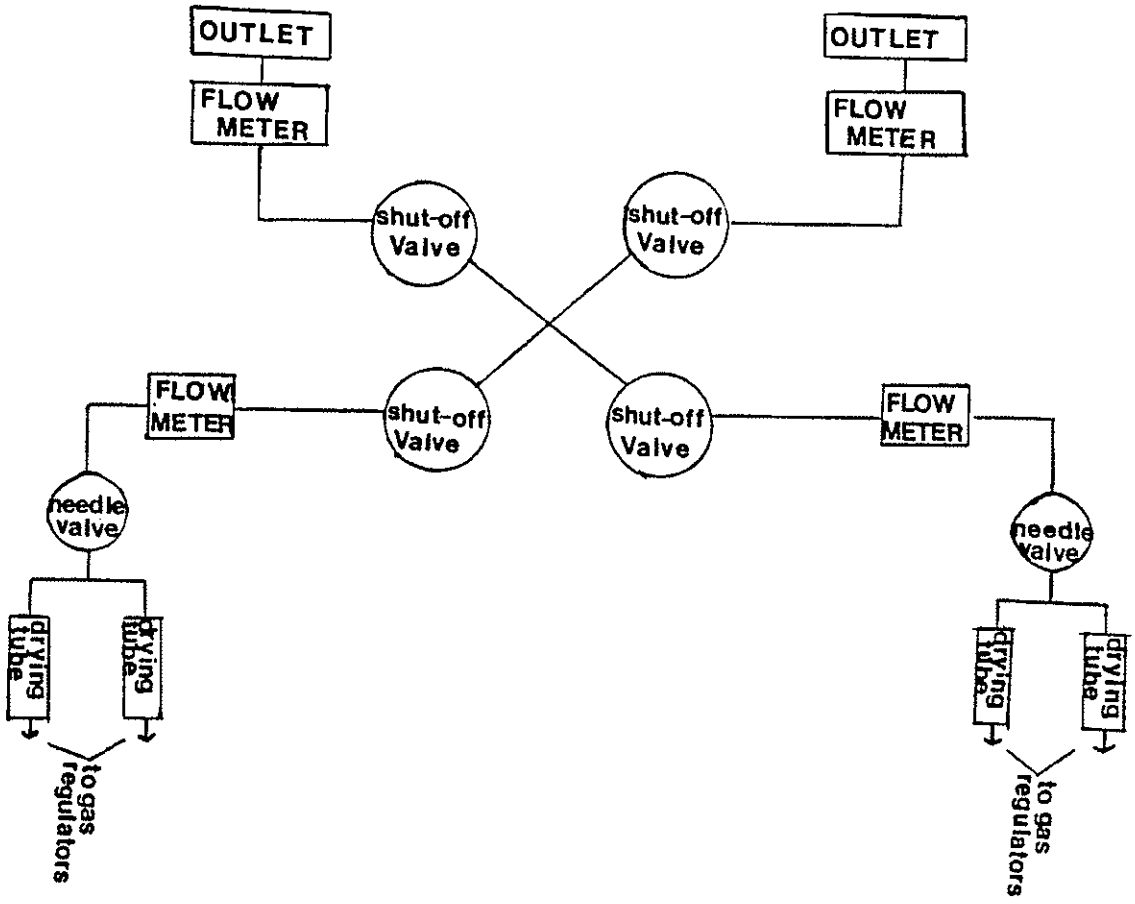
OUTLET
FLOW METER
OUTLET
FLOW METER
shut-off Valve
shut-off Valve
FLOW METER
shut-off Valve
shut-off Valve
FLOW METER
needle valve
needle valve
drying tube
drying tube
drying tube
drying tube
to gas regulators
to gas regulators

allow four cylinders of gas could be simultaneously connected. Standard brass Swagelock and pipe fittings were used for all connections. Two outlets were plumbed so that two independent experiments could be on the table. Silica gel drying tubes made by Henry, model VV403-1/4, were installed at the inlet side of the setup to dry the gas before reaching the reactor. Needle valves were used to control gas flowrates.

Hastings-Teledyne Raydist mass flow meters were used to measure all gas flowrates. These meters were calibrated over a range of 0-50 sccm for air. The indicated flowrate was multiplied by a correction factor of 1.38 supplied by the manufacturer to correct the meter reading when neon was used as carrier gas. This was necessary since the flow meter operates on the principle of thermal conductivity.

The reactor was heated in a Lindberg Hevi-Duty SB tube furnace. A Soltec model 4101 digital thermometer was connected to the furnace thermocouple for direct temperature read-out.

Ultra high purity neon was obtained from Scientific Gas Products, Inc. The nitrogen ($^{14}N_2$), (99.99%) purchased from Air Products. Prochem supplied the $^{15}N_2$, (99.6 atom percent) and the $^{18}O_2$,(99.4 atom percent). Isotec provided $^{18}O_2$ and $^{15}N_2$, each with a purity of 99 atom percent.

Procedure

The experimental procedure was to pack a 45 centimeter long, seven millimeter i.d. quartz tube with the desired material to be investigated and place it in the furnace. Stainless steel filters were positioned at the inlet and the outlet side of the tube to insure that none of the fine powder would escape into either the mass spectrometer or the mass flow meters. It was then connected into the flow system.

The reactor was pretreated, under neon flow conditions, by heating to 1100°C. A cool down cycle was also under neon flow. When the temperature of the reactor had fallen below 100°C a mass spectrum of the neon effluent was obtained as shown in Figure 3 to demonstrate completeness of outgassing and the absence of leaks. For the experimental run a mixture of approximately 2% of the selected test gas in neon was allowed to flow through the column. Mass spectra were then obtained as a function of temperature. The temperature was raised in 100°C increments to the desired maximum temperature and data taken at several flowrates. This procedure was carried out for both oxygen and nitrogen and their respective isotopes.

FIGURE 3

SPECTRUM OF NEON EFFLUENT

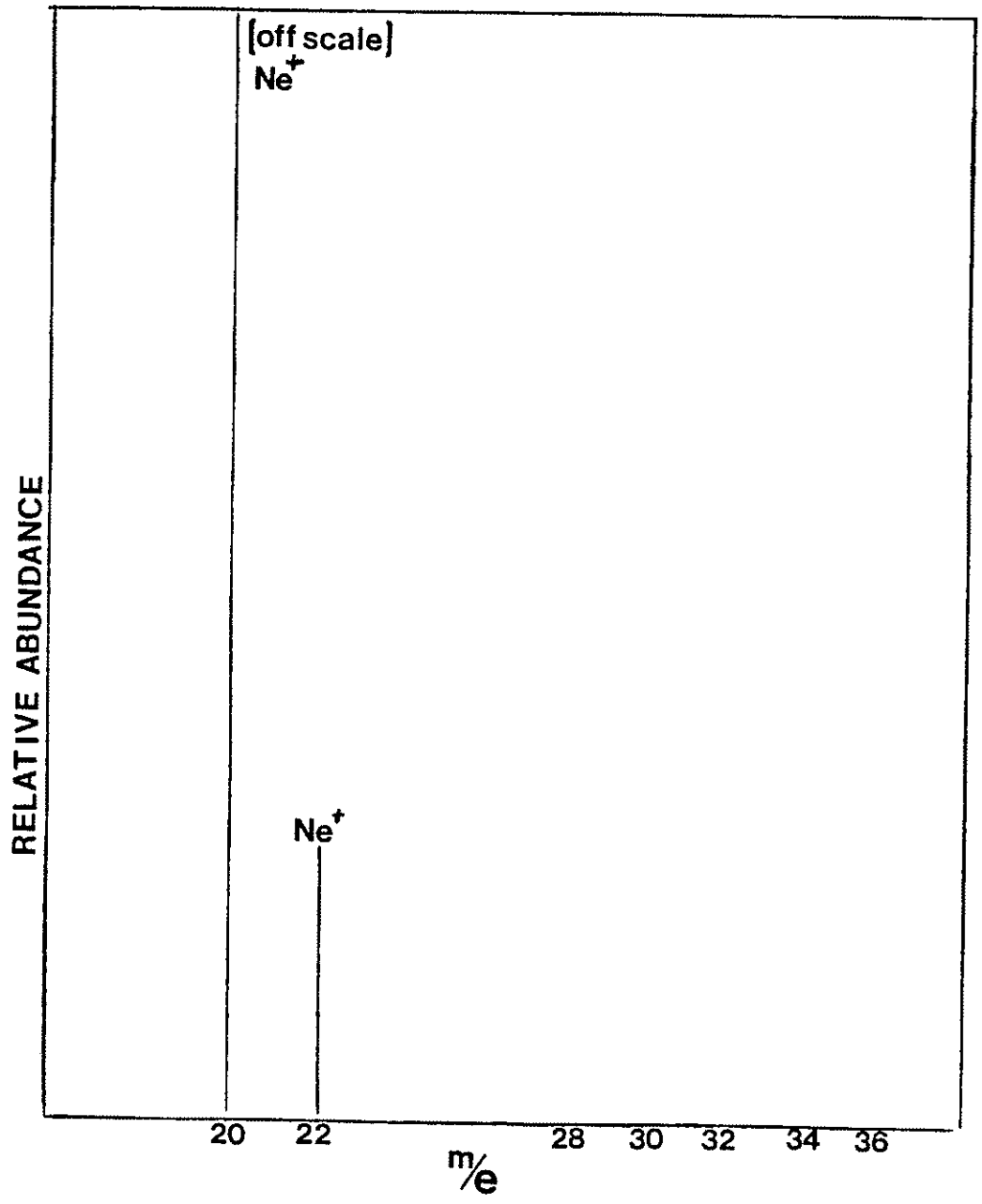
(off scale)
Ne^+
Ne^+
RELATIVE ABUNDANCE
20
22
28
30
32
34
36
m/e

Flowmeters were positioned both at the inlet and outlet side for monitoring gas flow to assure a leak-free system. The net flow rate was always maintained greater than the 4.2 ml/min pumping speed of the inlet capillary. This was necessary to insure that no air was introduced into the system and that the excess volume was vented to the atmosphere.

The mass spectrum was scanned through a mass-to-charge range from 12 to 40 amu. The ion peaks for the inert gas as well as the peaks of test gas and product were monitored. Scanning below 20 amu allowed the monitoring of the water peak.

For kinetic data at least two temperatures were selected under flow conditions where the reaction was still in the first half-life. The temperature was set and the flow rate changed. Flow rates ranged from 9 sccm to 45 sccm. At least five flowrates were selected at each temperature. A mass spectrum collected at each point was used to calculate the amount of gas reacted.[14,15]

When a mixture of $^{16}O_2$ and $^{18}O_2$ in neon was used the reaction could be monitored by the appearance of mass-to-charge (m/e) 34 where the oxygen molecules had dissociated and recombined forming the product molecule of $^{16}O\ ^{18}O$. These spectra are shown in Figures 4 and 5. In this set of experiments the

FIGURE 4

SPECTRUM OF $^{16}O_2$ $^{18}O_2$ IN NEON

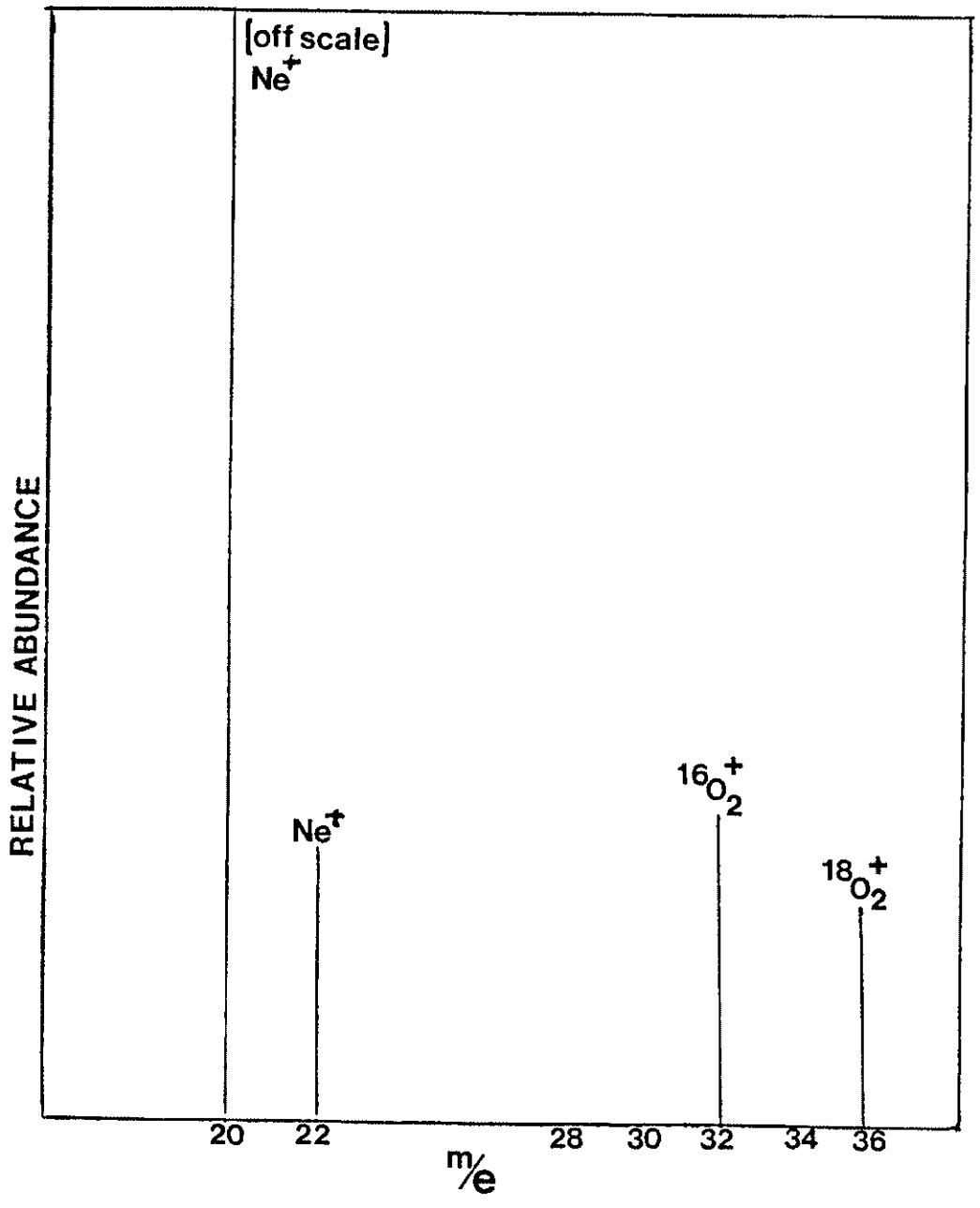
[off scale]
Ne^+
RELATIVE ABUNDANCE
Ne^+
$^{16}O_2^+$
$^{18}O_2^+$
20
22
28
30
32
34
36
m/e

FIGURE 5

SPECTRUM SHOWING APPEARANCE OF M/E 34

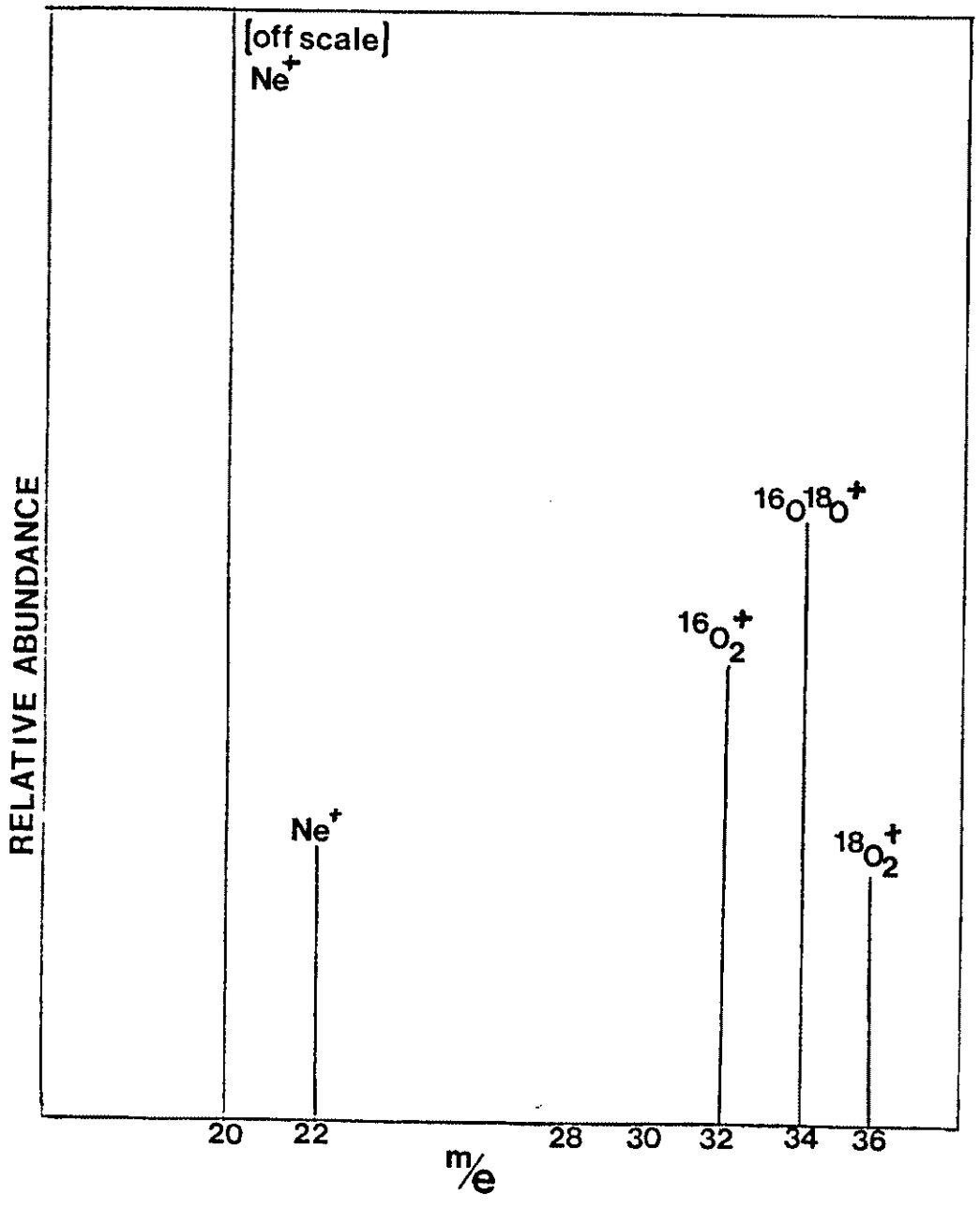
[off scale]
Ne+
RELATIVE ABUNDANCE
16O18O+
16O2+
Ne+
18O2+
20
22
28
30
32
34
36
m/e

temperature was increased in approximately 100°C increments to determine the extent of reaction as a function of temperature.

When a mixture of $^{18}O_2$ in neon was used alone it was possible to monitor exchange with the surface of the oxides being used. Appearance of m/e 34 was only possible if the oxide surface of the material actually participated in the reaction as opposed to merely providing a surface upon which the reaction could take place. A spectrum of $^{18}O_2$ in neon is shown in Figure 6, and the appearance of m/e 34 is seen in Figure 7 demonstrating that exchange with the oxide surface does take place at these temperatures.

For experiments with nitrogen, the isotopes $^{14}N_2$ and $^{15}N_2$ in neon were used. The initial spectrum of the nitrogen mixture can be seen in Figure 8. At 1100°C there was no scrambling as no mass compositional change was observed. If a reaction had occurred m/e 29 would have appeared.[16,17]

Experimental Data

Oxygen-16 and Oxygen-18 Blank

As in any quantitative chemistry experiment a blank run was necessary to determine if any reaction would occur and if so to what extent it occurred.

A routine conditioning cycle was employed at the

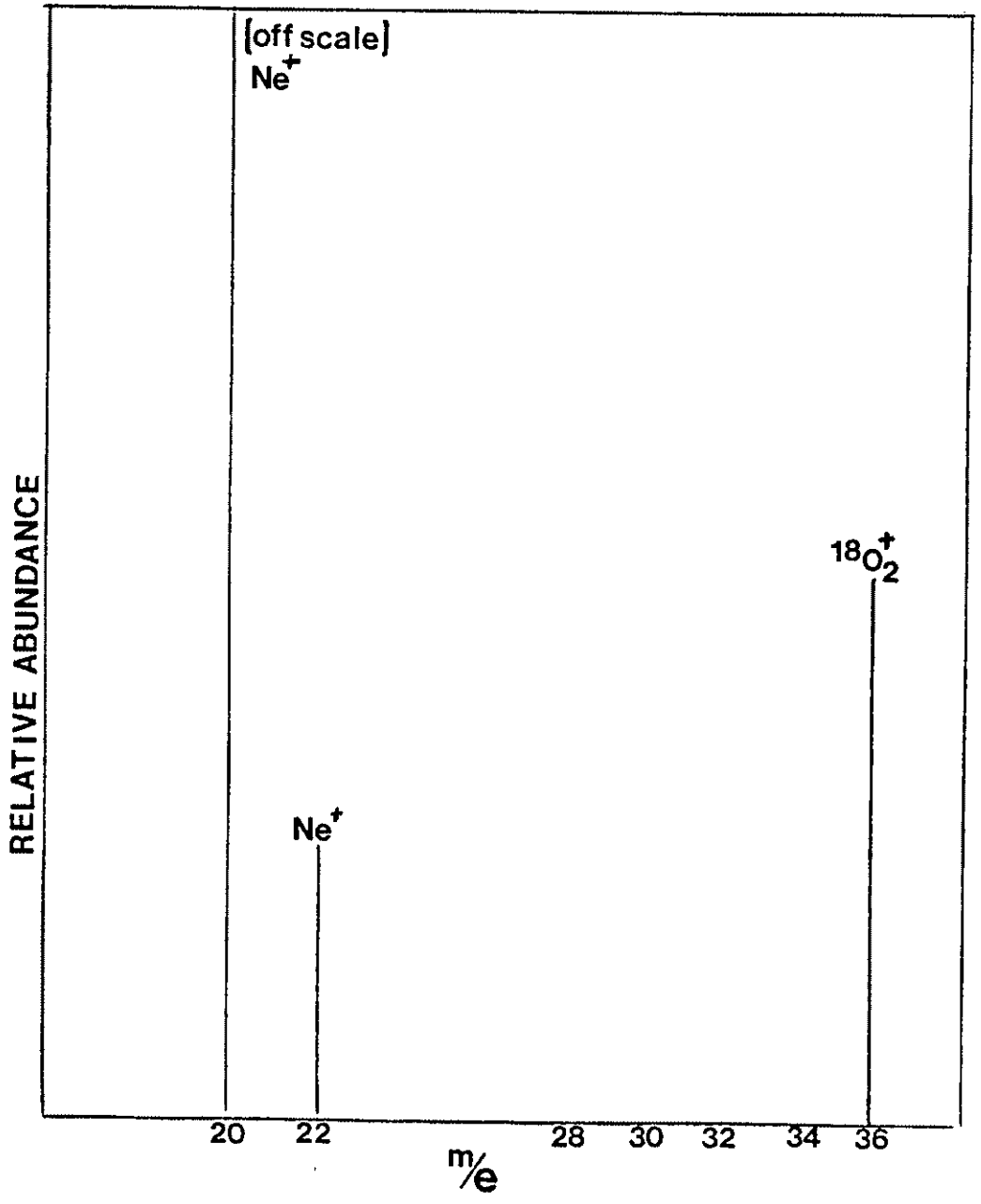
[off scale]
Ne+
Ne+
18O2+
RELATIVE ABUNDANCE
20
22
28
30
32
34
36
m/e

FIGURE 7

SPECTRUM SHOWING ISOTOPIC EXCHANGE WITH THE SURFACE

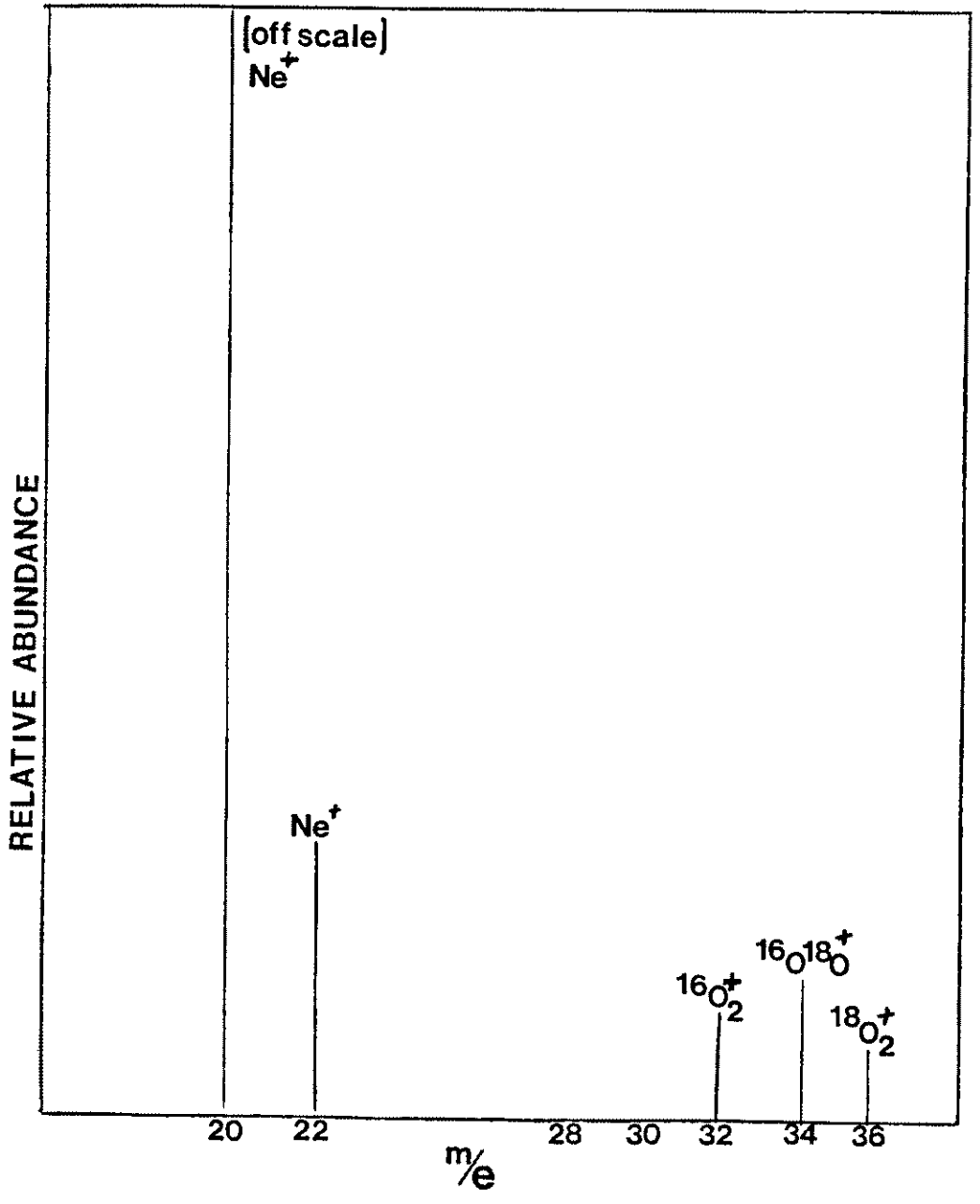
[off scale]
Ne+
Ne+
16O18O+
16O2+
18O2+
RELATIVE ABUNDANCE
20
22
28
30
32
34
36
m/e

FIGURE 8

SPECTRUM OF $^{14}N_2$ $^{15}N_2$ IN NEON

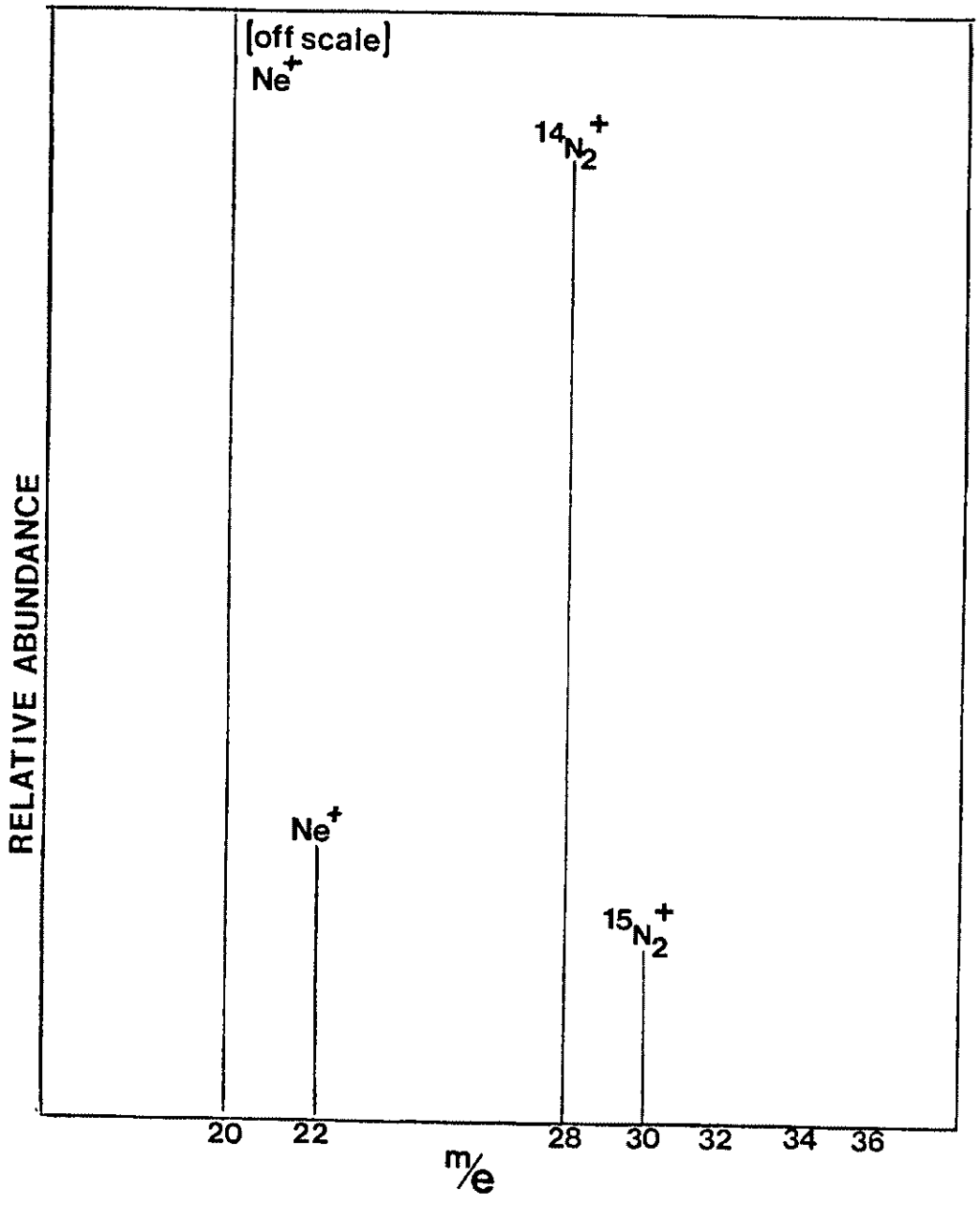
[off scale]
Ne^+
$^{14}N_2^+$
Ne^+
$^{15}N_2^+$
RELATIVE ABUNDANCE
20
22
28
30
32
34
36
m/e

beginning of each run. The temperature of the reactor was raised to 1100°C under neon flow and allowed to return to room temperature still under neon flow. The gas mixture was then introduced. A 2.6% $^{16}O_2$ and 1.8% $^{18}O_2$ mixture in neon was passed through the empty quartz tube. Under extremely high gain conditions appearance of m/e 34 was observed at approximately 700°C. It was determined, however, that the reaction on the surface of the tube was negligible since m/e 34 was not observed under normal operating conditions.

Reaction of Oxygen-16 and Oxygen-18 on Quartz Wool

Since quartz wool was to be used to plug the ends of the packed tube, it was decided to examine the quartz wool alone to see what reaction might take place. Fully packed there was some reaction occurring, but with the small amount being used in subsequent experiments and under normal operating conditions the contribution of this reaction was negligible. These data are graphically shown in Figure 9.

Oxygen-16 and Oxygen-18 on Crystalline Quartz

A quartz tube was packed with 14.16g of quartz powder. The conditioning cycle was performed. A mixture of 2.6% $^{16}O_2$ and 1.8% $^{18}O_2$ in neon was passed through the reactor and the temperature was raised.

FIGURE 9

ISOTOPIC OXYGEN EXCHANGE ON QUARTZ WOOL

$$^{16}O_2(G) + {}^{18}O_2(G) + Si^{16}O_2(S) \longrightarrow 2\ {}^{16}O^{18}O(G) + Si^{16}O_2(S)$$

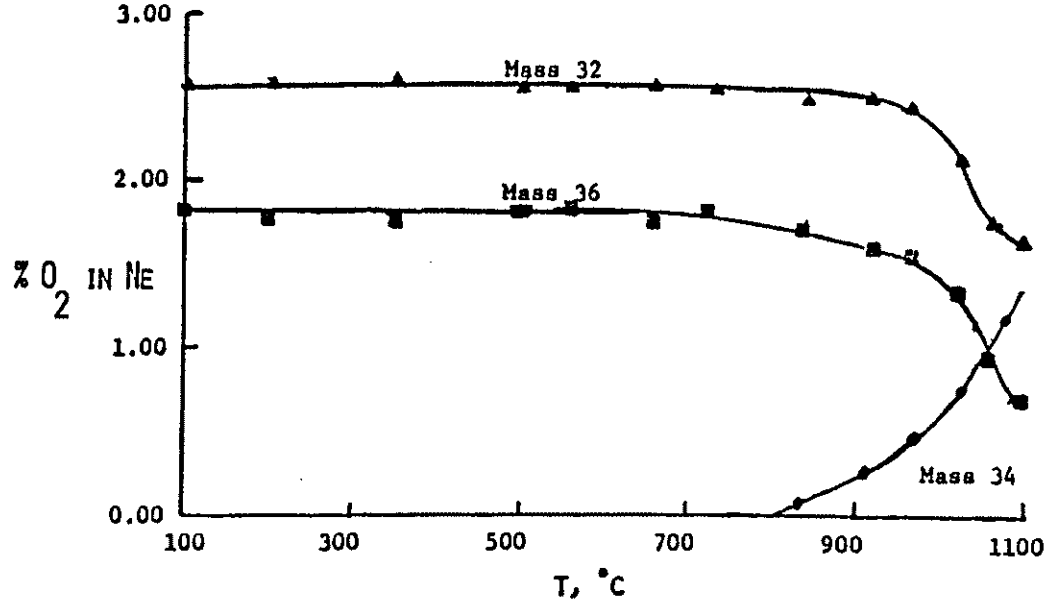

The disappearances of m/e 32 and m/e 36 were monitored as well as the appearance of m/e 34. Between 700°C and 800°C m/e 34 appeared. The intensity continued to increase until the maximum temperature was reached. These data are shown in Figure 10.

Oxygen-16 and Oxygen-18 on Amorphous Silica

A fused quartz tube was packed with 15.41g of amorphous silica. A 2.6% $^{16}O_2$ and 1.8% $^{18}O_2$ in neon mixture was passed through the packing. The temperature was raised gradually to 1100°C. M/e 34 appeared at 800°C. It was later learned that the amorphous silica tended to take on some crystalline characteristics when heated to temperatures above 900°C.[18] The results of subsequent runs are shown in Figure 11.

FIGURE 10

ISOTOPIC OXYGEN SCRAMBLING ON CRYSTALLINE QUARTZ

$$^{16}O_2(G) + {}^{18}O_2(G) + Si^{16}O_2(S) \longrightarrow 2\,{}^{16}O^{18}O(G) + Si^{16}O_2(S)$$

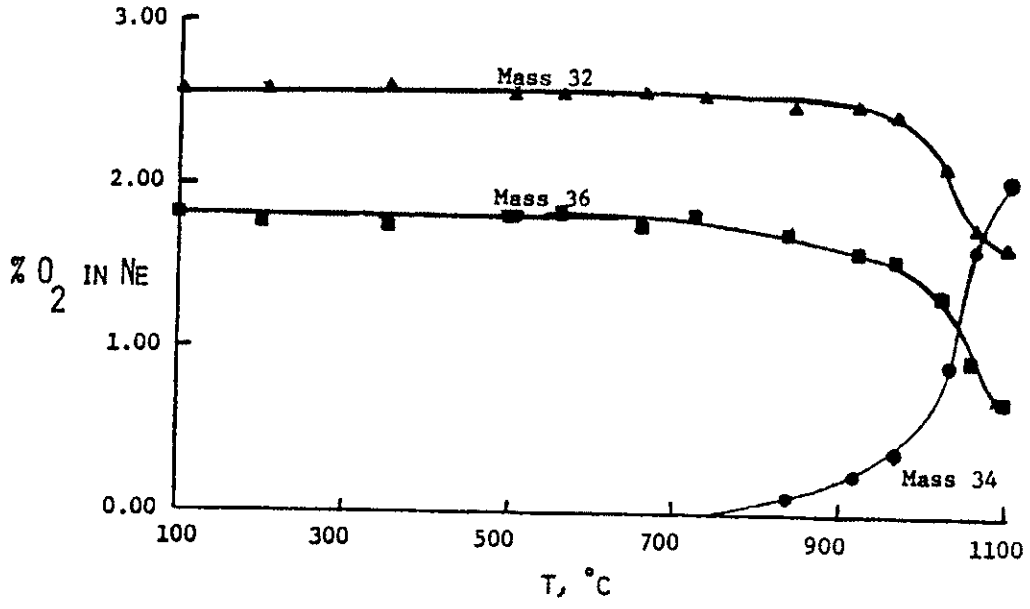

FIGURE 11

ISOTOPIC OXYGEN SCRAMBLING ON AMORPHOUS SILICA

$$^{18}O_2(G) + Si^{16}O_2(S) \longrightarrow {}^{16}O^{18}O(G) + Si^{16}O^{18}O(S)$$

$$^{18}O_2(G) + {}^{16}O_2(G) \xrightarrow[SiO_2(s)]{} 2\ {}^{16}O^{18}O(G)$$

$$^{16}O^{18}O(G) + Si^{16}O_2(S) \longrightarrow {}^{16}O_2(G) + Si^{16}O^{18}O(S)$$

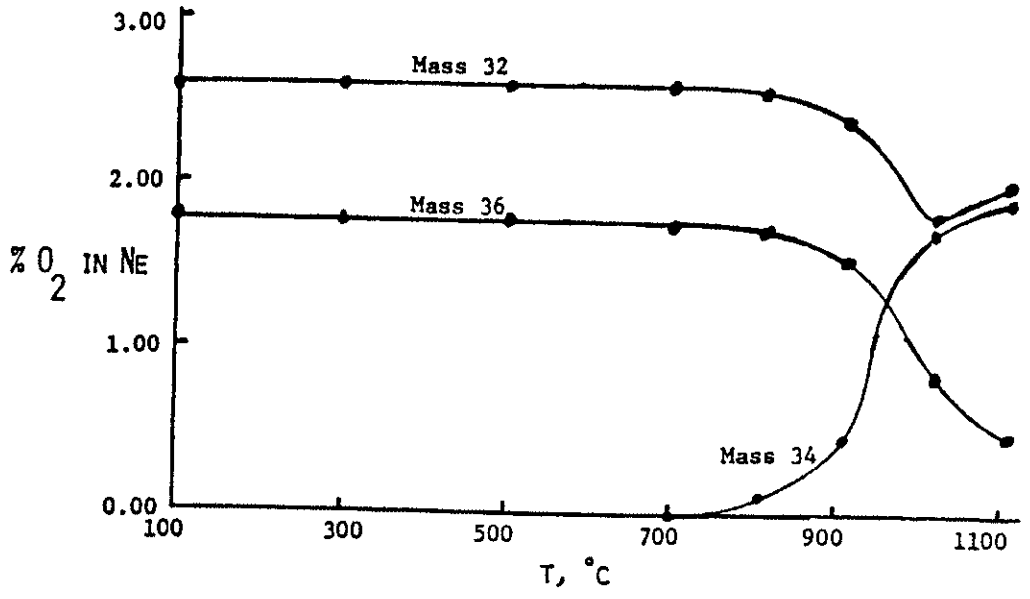

Oxygen-16 and Oxygen-18 on Borosilicate Glass Wool

Borosilicate glass wool was packed into the quartz tube. The temperature could not be raised to 1000°C due to its low softening point. The same mixture of $^{16}O_2$ and $^{18}O_2$ in neon was used as in the previous experiment. As can be seen in Figure 12, the appearance of m/e 34 occurred at 500°C. This was much lower than any of the other materials examined to this point.

Oxygen-18 Blank

A blank was run with just 1.94% $^{18}O_2$ in neon to determine if there would be any exchange with the surface of the quartz tube. The temperature was raised to 1100°C with no appearance of m/e 34 occurring.

Oxygen-18 on CrystallineQuartz

A fused quartz tube was packed with 16.64g of crystalline quartz. After conditioning, 1.94% $^{18}O_2$ in neon was passed through the reactor. Mass-to-charge 34 appeared at 900°C. There was a very low percentage of conversion up to 1100°C as shown in Figure 13.

FIGURE 12

ISOTOPIC OXYGEN EXCHANGE ON GLASS WOOL

$$^{16}O_2(G) + {}^{18}O_2(G) \xrightarrow[SiO_2(s)]{} 2\ {}^{16}O{}^{18}O(G)$$

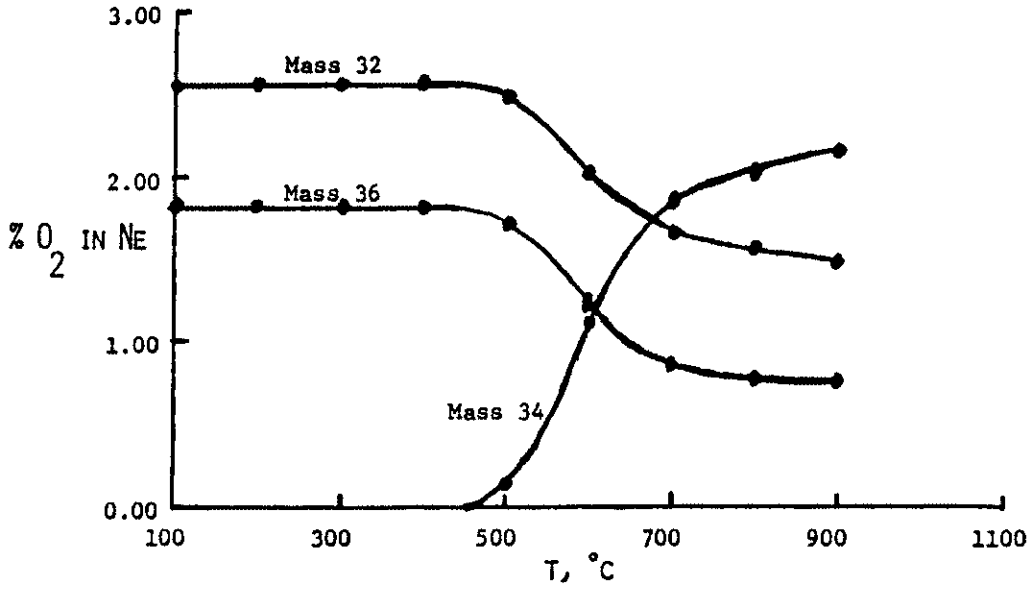

FIGURE 13

ISOTOPIC OXYGEN EXCHANGE ON CRYSTALLINE QUARTZ

$$^{18}O_{2\,(G)} + Si^{16}O_{2\,(S)} \longrightarrow {}^{16}O^{18}O_{(G)} + Si^{16}O^{18}O_{(S)}$$

$$^{16}O^{18}O_{(G)} + Si^{16}O_{2\,(S)} \longrightarrow {}^{16}O_{2\,(G)} + Si^{16}O^{18}O_{(S)}$$

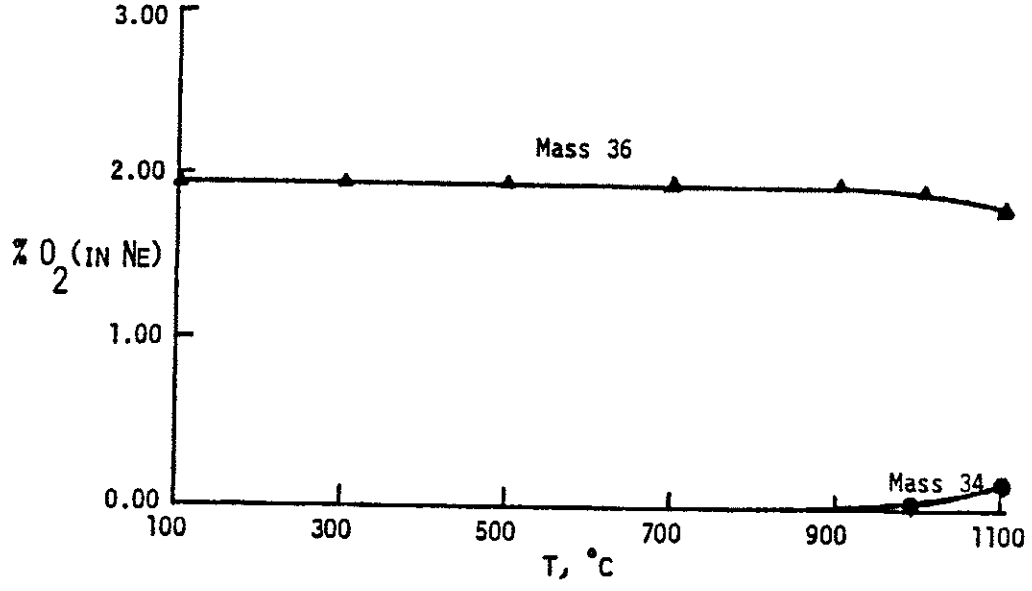

Oxygen-18 on Amorphous Silica

With 15.41g of amorphous SiO_2 packed in the quartz tube, m/e 34 appeared at 700°C indicating exchange with the surface at a temperature 200°C lower than with the crystalline quartz material. These data are shown in Figure 14.

Oxygen-18 in Pyrex tube and Borosilicate Glass Wool

Exchange with the surface occurred at approximately 800°C (near the softening point) when $^{18}O_2$ in neon was passed through the borosilicate glass wool. As will be discussed later, this was a significant experiment when the kinetics observed were being considered.

Reactions with Nitrogen

Nitrogen-14 and Nitrogen-15 on Crystalline Quartz and Amorphous Silica

Crystalline quartz was packed into a quartz tube and, after conditioning, a mixture of 6.5% $^{14}N_2$ and 1% $^{15}N_2$ in neon was passed through it and mass spectrometrically monitored. No m/e 29 was observed. There was no scrambling at the surface even at 1100°C.

The same procedure was carried out with the amorphous silica, and again there was no scrambling

FIGURE 14

ISOTOPIC OXYGEN EXCHANGE ON AMORPHOUS SILICA

$$^{18}O_{2\,(G)} + Si^{16}O_{2\,(S)} \longrightarrow {}^{16}O^{18}O_{(G)} + Si^{16}O^{18}O_{(S)}$$

$$^{16}O^{18}O_{(G)} + Si^{16}O_{2\,(S)} \longrightarrow {}^{16}O_{2\,(G)} + Si^{16}O^{18}O_{(S)}$$

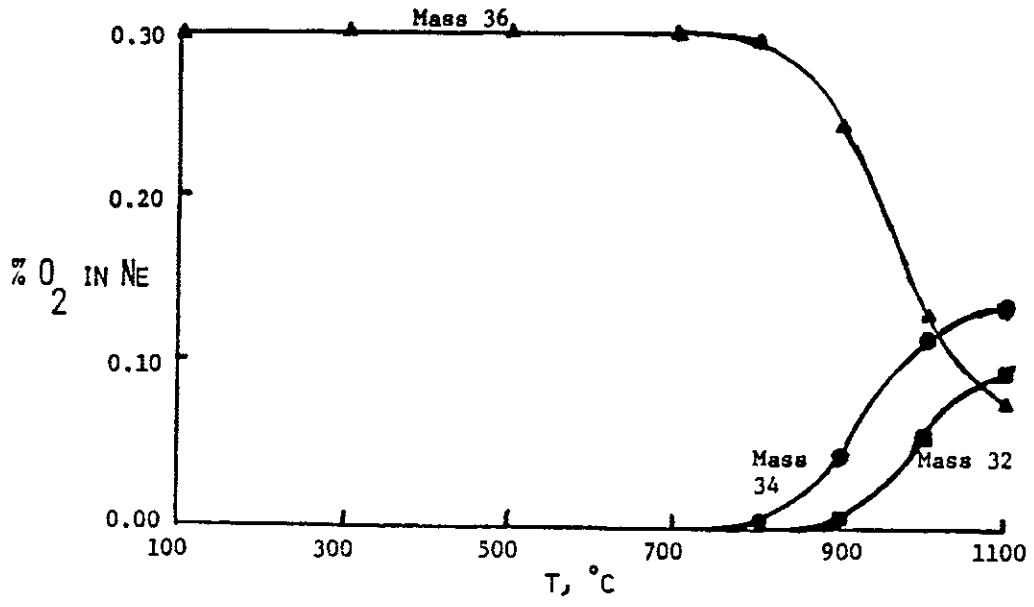

reaction at the surface of this material. It was demonstrated that there were no catalytic effects on these two surfaces toward nitrogen at these temperatures and no further experimentation was carried out with the nitrogen.

Crystallographic Studies

X-ray diffraction was used to determine whether the samples were crystalline or amorphous. This was done at the X-ray diffraction laboratory at NASA, Langley. The samples were also examined with a polarized light microscope.

The quartz was found to be crystalline by both the diffraction and microscopic techniques. The Davidson silica was found to be amorphous by both techniques. Under polarized light the quartz wool was clearly anisotropic proving it to be crystalline in character.

Kinetic Studies

Kinetic data were taken for the reactions of molecular oxygen with the oxide surfaces of amorphous silica and crystalline quartz. These data were taken to allow a plot of concentration versus residence time at a constant temperature. Data for the kinetic studies were obtained at 1000^{o}C and 1100^{o}C using the

crystalline and amorphous materials. These temperatures were selected because exchange was observed to occur. Two temperatures one hundred degrees apart were selected so that rate constants and the activation energy values could be more accurately determined. After the rate law was found and the rate constants evaluated, the energy of activation (E_a) was determined from a form of the Arrhenius equation as follows:

$$\ln k_2/\ln k_1 = E_a(T_2-T_1) \;/\; RT_1T_2 \;.$$

The frequency factor s was calculated from the Arrhenius equation in standard form:

$$k = se^{-E_a/RT}$$

The residence time (actual time spent in reactor bed) was determined as in kinetic flow experiments of others as follows:[19]

$$t = (VV/FR)x(293K/T)x(60sec/min)$$

where t = time in seconds

VV = void volume in ml

FR = mass flow rate at 293K in ml

T = absolute temperature of reactor

Since some function of the $^{18}O_2$ concentration in the void volume of the reactor bed was to be plotted versus residence time both of these parameters had to be determined or calculated. To calculate the $^{18}O_2$

concentration in the void volume of the material of interest it was assumed that the pressure in the reactor was one atmosphere and the subsequent calculation of concentration was obtained from the known partial pressures as follows:

$$^{18}O_2 = P_{O2}/(RT)$$

where R = 0.08205 (l-atm)/mol K and T is the absolute temperature.[20]

To determine the partial pressure of the individual components, the percentage composition of the component of interest was used. A calculation relative to the neon m/e 22 was made. Since 2.68% mole percent of $^{18}O_2$ was the initial concentration the partial pressure was therefore 0.0268 atmospheres. In mass spectrometry the intensity of a peak is directly proportional to its partial pressure so the partial pressure may be readily measured mass spectrometrically. Thus at any reactor temperature calculations for other concentrations may easily be made.

In order to calculate the residence time, the void volume of the packing had to be determined. Several options were available, but it was decided that the density method was the best choice. A volumetric flask was filled to the mark with the test material and weighed. Carbon tetrachloride was added

and using the known density of carbon tetrachloride, 1.5867g/cc, (from CRC Handbook of Chemistry and Physics) the void volume was calculated. The same procedure was used for both the crystalline quartz and amorphous silica. The void volume was 6.11ml for the amorphous silica and 4.23ml for the crystalline quartz material under packing conditions used in the reaction tube. Data obtained for the kinetic studies are tabulated in Tables II - V.

Table II.

Kinetic Data for Oxygen-18 on Amorphous Silica at 1000°C

Temp °C	FR SCCM	time sec	% m/e 32	% m/e 34	% m/e 36	m/e 36 $[C]x10^4$	m/e 36 $[C]^{-1}x10^{-3}$
1000	8.5	9.93	0.27	0.91	1.52	1.46	6.87
1001	17.1	4.93	0.13	0.66	1.89	1.81	5.53
1000	24.2	3.49	0.08	0.48	2.12	2.03	4.93
998	32.0	2.64	0.06	0.37	2.25	2.06	4.63
1000	43.9	1.92	0.05	0.30	2.33	2.23	4.48

Table III.

Amorphous Silica at 1100°C

Temp °C	FR SCCM	time sec	% m/e 32	% m/e 34	% m/e 36	m/e 36 $[C]\times10^{4}$	m/e 36 $[C]^{-1}\times10^{-3}$
1103	10.3	7.57	0.37	1.19	1.12	9.94	10.06
1108	19.4	5.00	0.27	1.06	1.35	1.19	8.40
1106	28.6	2.72	0.15	0.83	1.70	1.50	6.65
1111	37.6	2.06	0.10	0.67	1.91	1.68	5.95
1102	50.3	1.55	0.07	0.53	2.08	1.84	5.44

Table IV.

Kinetic Data of Oxygen-18 on Crystalline Quartz at 1000°C

Temp °C	FR SCCM	time sec	% m/e 32	% m/e 34	% m/e 36	m/e 36 $[C]\times10^4$	m/e 36 $[C]^{-1}\times10^{-3}$
1010	9.9	5.94	0.50	0.24	2.39	2.28	4.38
1006	9.9	5.96	0.04	0.23	2.41	2.29	4.36
1010	19.5	3.01	0.03	0.16	2.49	2.36	4.24
1005	19.5	3.03	0.03	0.16	2.50	2.38	4.20
1003	28.4	2.08	0.04	0.12	2.52	2.40	4.16
1010	28.4	2.07	0.04	0.13	2.53	2.40	4.17
1008	40.1	1.47	0.03	0.11	2.54	2.42	4.14
1003	40.1	1.47	0.04	0.11	2.53	2.42	4.14

Table V.

Kinetic Data of Oxygen-18 on Alpha Quartz at 1100°C

Temp °C	FR SCCM	time sec	% m/e 32	% m/e 34	% m/e 36	m/e 36 $[C]\times10^{4}$	m/e 36 $[C]^{-1}\times10^{-3}$
1112	10.0	5.87	0.11	0.75	1.83	1.61	6.22
1113	10.0	5.87	0.11	0.76	1.81	1.59	6.28
1112	20.1	2.71	0.03	0.38	2.27	2.00	5.01
1111	20.1	2.71	0.04	.033	2.31	2.03	4.92
1113	30.4	1.79	0.03	0.28	2.37	2.08	4.80
1111	30.4	1.79	0.03	0.29	2.36	2.08	4.81
1116	43.8	1.24	0.02	0.24	2.42	2.12	4.71
1115	43.8	1.24	0.02	0.25	2.41	2.11	4.73

CHAPTER III

RESULTS AND DISCUSSION

The graphs of the kinetic data for a second order rate law at 1000°C and 1100°C for amorphous silica and crystalline quartz are shown in Figures 15 and 16. The graphs clearly demonstrate second order kinetics for the $^{18}O_2$ in the exchange reaction between $^{18}O_2$ and the oxygen in the oxide surfaces. It would have been better if a higher temperature could have been used for the crystalline quartz, because at 1000°C there was little activity, but there was a temperature limitation of 1100°C for the experimental system. Both reactions were consistent with a second order mechanism equation ($-dC/dt = k\ C^{2}$). The rate constants for reactions on amorphous silica and crystalline quartz were 2.2×10^{2} L/mol/sec and 2.0×10^{2} L/mol/sec respectively. The frequency factor for amorphous silica was 1.35×10^{9} L/mol/sec with an activation energy of 35.3kcal/mol. On the crystalline quartz, the frequency factor was 4.51×10^{12} L/mol/sec and the activation energy was 65.2 kcal/mol.

The amorphous material on an initial run exhibited catalytic activity much lower than on a

FIGURE 15

GRAPH OF KINETIC STUDIES DATA ON AMORPHOUS SILICA

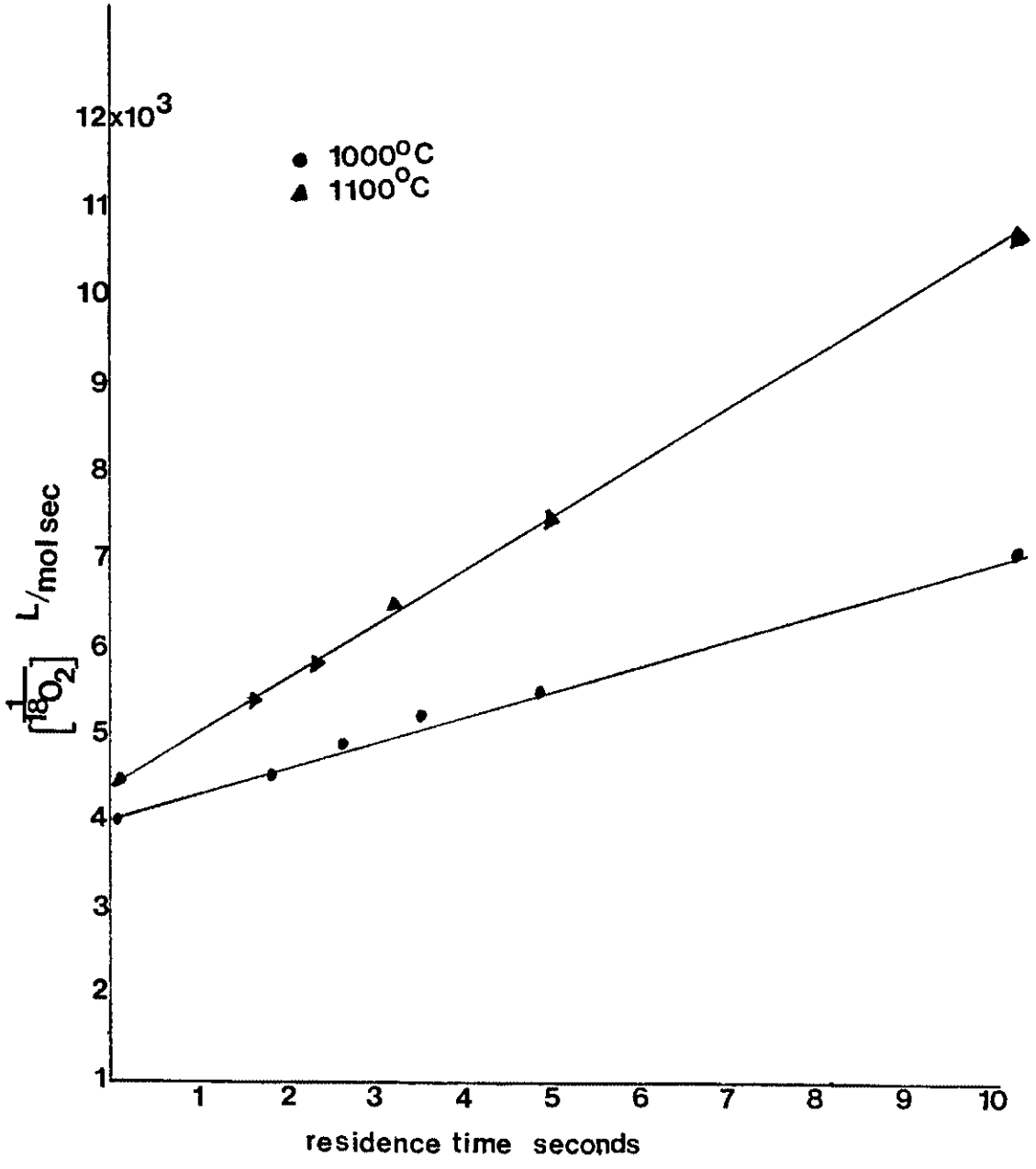
12x10^3
11
10
9
8
7
6
5
4
3
2
1
● 1000°C
▲ 1100°C
1/[18O2] L/mol sec
1
2
3
4
5
6
7
8
9
10
residence time seconds

FIGURE 16

GRAPH OF KINETIC STUDIES DATA ON CRYSTALLINE QUARTZ

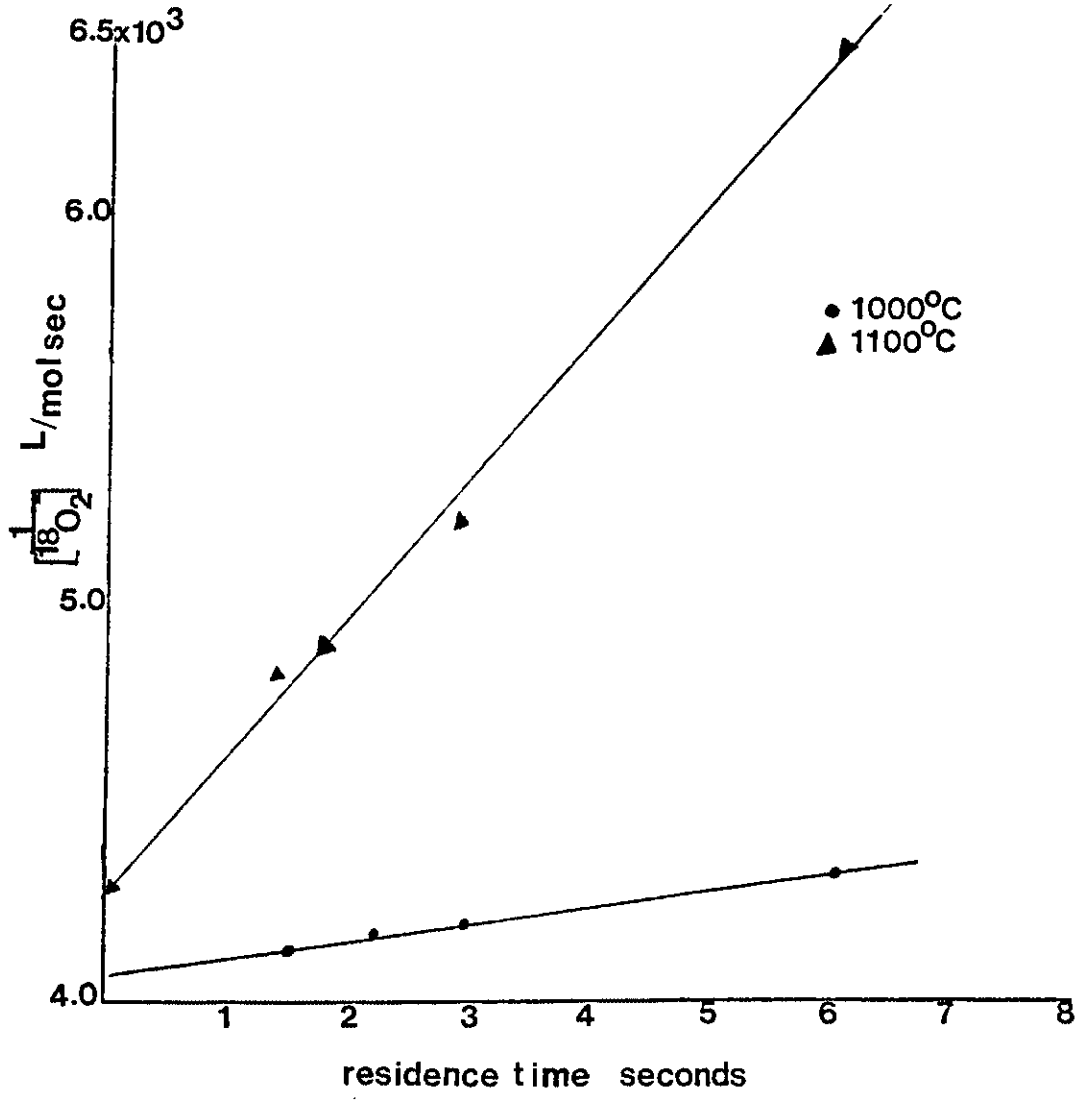
6.5x10^3
6.0
5.0
4.0
L/mol sec
1/[18O2]
1000°C
1100°C
1
2
3
4
5
6
7
8
residence time seconds

second run of the same material. As was discussed earlier non-crystalline quartz will devitrify and become more crystalline in character when used above the 1000°C range. This perhaps explains why the initial experimental data for the amorphous material could not be repeated on subsequent runs probably due to a decrease in active sites as the amorphous material is exposed to the higher temperatures.

Adsorption of a gas by a solid may occur by two mechanisms. This first mechanism is physical adsorption. This is a weak binding of the gas to the surface by Van der Waal type forces and is easily reversed upon heating. Another type of physical adsorption is condensation of the gas in the pores of the surface and is much more difficult to remove by heating.[21]

The second mechanism, chemisorption is actually a reaction. Adsorption of this type is very energetic and is not readily removed reversibly. These chemisorbed atoms are the atoms that are thought to participate in the atom recombination process.[22,23]

It has been shown that materials high in "percent d character" with regard to the number of filled d orbitals tend to be more catalytic. This supports experimental data where nickel, which is high in "percent d character" is highly catalytic and quartz,

which has a low "percent d character" is relatively non-catalytic. Is is still not clearly understood why "d" orbitals are more effective than "s" or "p" orbitals.

In these experiments, the scrambling exchange reaction takes place only at elevated temperatures. For the crystalline quartz, the scrambling begins around 900°C. If the equilibrium crystallographic forms of this material are examined, it can be seen that:[24]

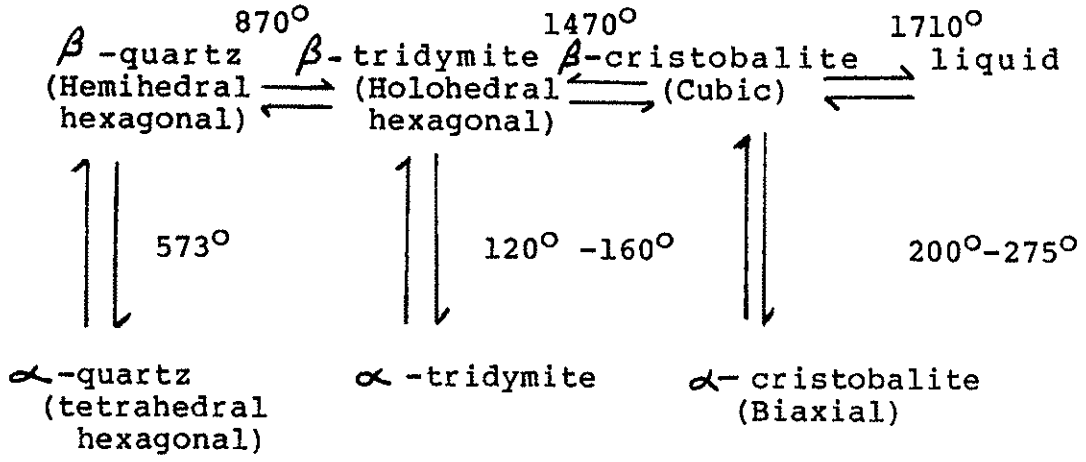

The transition of β-quartz to β-tridymite may be a key to the active site question. Interconversion of quartz and tridymite require bond breaking and remaking. If in the process there is some new type of surface not seen below the 870°C temperature, it is possible that this does play an important role in the catalytic activity of the material.

Gray and Darby[25] have studied the reaction of O_2 on metal oxides at low pressures. It is not known how this compares with higher pressures, but in their experiments the slow step was desorption of O_2 and was second order.

It is well known that the SiO_2 exposed to the atmosphere has many hydroxyl groups rather than exposed oxygen atoms on the surface of the lattice structure. When heated, water is liberated when the hydroxyl groups decompose, leaving exposed surface ionic groups. The surface ionic groups are probably the active sites which allow adsorption of the oxygen molecules passing through the void volume of the material.

CONCLUSION

Isotopic exchange with the surface of these two oxides when the molecular species is used clearly obeys second order kinetics. Since this requires a bimolecular reaction the following mechanism is postulated:

$$A + {}^{18}O_2 \xrightarrow{k_1} A^{18}O_2$$

$$A^{18}O_2 + {}^{18}O_2 \xrightarrow{k_2} B + {}^{18}O_2 + {}^{16}O{}^{18}O$$

$$\frac{d(B)}{dt} = k_2({}^{18}O_2)(AO_2)$$

$$K = \frac{(A^{18}O_2)}{(A)({}^{18}O_2)}$$

$$\text{therefore, } \frac{d(B)}{dt} = k_2K(A)({}^{18}O_2)^2$$

where, $A = Si^{16}O_2$ and $B = Si^{16}O^{18}O$.

For this mechanism the active sites are formed on the surface when the temperature is above that required for dehydroxylation. This allows chemisorption of the molecule of $^{18}O_2$ forming a bridged six-member ring structure upon which a subsequent collision of a second $^{18}O_2$ molecule results in oxygen isotope exchange. Since it appears that more uniformly structured materials yield the fewest

active sites, coding or doping with materials to deactivate these sites, would result in a composite that meets more of the requirements for an ideal non-catalytic overcoat for future re-entry vehicles.

BIBLIOGRAPHY

REFERENCES CITED

1. Sanders, H.J. Chem. Eng. News 1984, 62(28), 26.

2. Linnett, J.W. and Marsden, D.G. Proc. Ray. A. 1956, 234, 489;504.

3. Greaves, J.C. and Linnett, J.W. Trans. Faraday Soc. 1959, 4, 1323.

4. Greaves, J.C. and Linnett, J.W. TRANS. Faraday Soc. 1959, 55, 1346.

5. Rahman, M.L. and Linnett, J.W. TRANS. Faraday Soc. 1971, 67, 170.

6. Kistiakowsky, G.B. J. Chem. Phys. 1956, 25, 457.

7. Kistiakowsky, G.B. and Volpi, G.G., J. Chem. Phys. 1957, 27, 114.

8. Klein, F.S. and Herron, J.T. J. Chem. Phys. 1964, 41, 1285.

9. Elly, D.D., Frankenburg, W.G., Komarowsky, V.I., "Advances in Catalysis", 1st Ed; Academic Press Inc: New York, 1959.

10. Dickens, P.G. and Sutcliffe, M.S. TRANS. Faraday Soc. 1964, 60, 1272.

11. Gibbs, R.E., Proc. Ray. A. 1925, 110A, 443.

12. Bragg, W. and Gibbs, R.E., Proc. Ray. A. 1925, 109A, 405.

13. Gibson, J. Chem. Phys. 1928, 32, 1206.

14. Harris, G.M. J. Phys. & Colloid. Chem. 1947, 51, 505.

15. Benton, A. J. Am. Chem. Soc. 1931, 53, 2984.

16. Williams, E.L. J. Am. Cer. Soc. 1965, 48 190.

17. Sucov, E.W. J. Am. Cer. Soc. 1963, 46, 14.

18. Doremus, J. "Glass Science" 1st ed; John Wiley & Sons, Inc. New York, 1953.

19. Frost, A.A. and Pearson, R.G. "Kinetics and Mechanism", 1st ed; John Wiley & Sons, Inc. New York, 1953.

20. Alberty, R.A. and Daniels, R. "Physical Chemistry", 2nd ed: John Wiley & Sons, Inc. New York, 1962.

21. Hoening, C. University of Calif., 1953, "Oxygen Recombination Program" Report No. 2.

22. Scott, C.D. NASA Lyndon B. Johnson Space Center, July 1980, AIAA Report 80-1477.

23. Stewart, D.A. and Ratich, J.V. NASA Ames Research Center, June, 1981, AIAA Report 81-1143.

24. Cotton, F.A. and Wilkinson, G. "Advances Inorganic Chemistry" 1st ed; John Wiley & Sons, Inc. New York, 1962.

25. Gray, T.J. and Darby, P.W. J. Chem. Phys. 1956, 60, 201.